A Tsunami Forecast Model for Adak, Alaska

Christopher Chamberlin

NOAA Center for Tsunami Research

Pacific Marine Environmental Laboratory

DRAFT

September 2010

Introduction

The National Oceanic and Atmospheric Administration (NOAA) Center for Tsunami Research (NCTR) at the NOAA Pacific Marine Environmental Laboratory (PMEL) has developed a tsunami forecasting system for operational use by NOAA's two Tsunami Warning Centers located in Hawaii and Alaska (Titov *et al.*, 2005). The system is designed to efficiently provide basin-wide warning of approaching tsunami waves accurately and quickly. The system, termed Short-term Inundation Forecast of Tsunamis (SIFT), combines real-time tsunami event data with numerical models to produce estimates of tsunami wave arrival times and amplitudes at a coastal community of interest. The SIFT system integrates several key components: deep-ocean observations of tsunamis in real time, a basin-wide pre-computed propagation database of water level and flow velocities based on potential seismic unit sources, an inversion algorithm to refine the tsunami source based on deep-ocean observations during an event, and high-resolution tsunami inundation forecast models.

This report documents the development of a tsunami inundation forecast model covering the community of Adak, Alaska. This operational forecast model is designed for integration into the SIFT system.

Forecast Methodology

A high-resolution inundation model was used as the basis for development of a tsunami forecast model to operationally provide an estimate of wave arrival time, wave height, and inundation at Adak following tsunami generation. All tsunami forecast models are run in real time while a tsunami is propagating across the open ocean. The Adak model was designed and tested to perform under stringent time constraints given that time is generally the single limiting factor in saving lives and property. The goal of this work is to maximize the length of time that the community of Adak has to react to a tsunami threat by providing accurate information quickly to emergency managers and other officials responsible for the community and infrastructure.

The general tsunami forecast model, based on the Method of Splitting Tsunami (MOST), is used in the tsunami inundation and forecasting system to provide real-time tsunami forecasts at selected coastal communities. The model runs in minutes while employing high-resolution grids constructed by the National Geophysical Data Center. MOST is a suite of numerical simulation codes capable of simulating three processes of tsunami evolution: earthquake, transoceanic propagation, and inundation of dry land. The model has been extensively tested against a number of laboratory experiments and benchmarks (Synolakis *et al.* 2008) and was successfully used for simulations of many historical tsunami events. The main objective of a forecast model is to provide an accurate, yet rapid, estimate of wave arrival time, wave height, and inundation in the minutes following a tsunami event. Titov and González

(1997) describe the technical aspects of inundation model development, stability, testing, and robustness, and Tang *et al*. (2009) provide detailed forecast methodology.

A basin-wide database of pre-computed water elevations and flow velocities for unit sources covering worldwide subduction zones has been generated to expedite forecasts (Gica *et al.* 2008). As the tsunami wave propagates across the ocean and successively reaches tsunameter observation sites, recorded sea level is ingested into the tsunami forecast application in near real-time and incorporated into an inversion algorithm to produce an improved estimate of the tsunami source. A linear combination of the pre-computed database is then performed based on this tsunami source, now reflecting the transfer of energy to the fluid body, to produce synthetic boundary conditions of water elevation and flow velocities to initiate the forecast model computation.

Accurate forecasting of the tsunami impact on a coastal community largely relies on the accuracies of bathymetry and topography and the numerical computation. The high spatial and temporal grid resolution necessary for modeling accuracy poses a challenge in the run-time requirement for real-time forecasts. Each forecast model consists of three telescoped grids with increasing spatial resolution in the finest grid, and temporal resolution for simulation of wave inundation onto dry land. The forecast model utilizes the most recent bathymetry and topography available to reproduce the correct wave dynamics during the inundation computation. Forecast models, including the Adak model, are constructed for at-risk coastal communities in the Pacific and Atlantic Oceans. Previous and present development of forecast models in the Pacific (Titov *et al.* 2005; Tang *et al.* 2008; Wei *et al.* 2008; Titov 2009) have validated the accuracy and efficiency of each forecast model currently implemented in the real-time tsunami forecast system.

Model development

This section describes the tsunami model created for Adak, including background on the region, its tsunami event history, input data sources, and the process of model grid development.

Forecast area

The town of Adak, population 361 (2009 United States Census est.), is located on the northeast side of Adak Island. The island is part of the Andreanof Islands group of the Aleutian Islands. Adak is the southernmost population center in Alaska, and the largest population center in the Aleutian Islands west of Unalaska (Figure 1). There are no other towns or settlements on Adak Island outside of the town of Adak (Figure 2). The town's harbor, Sweeper Cove, is well-protected from weather, making it one of the safest harbors in the Aleutian Islands (United States Coast Pilot 2010).

During World War II, Adak was a major United States Navy supply and logistics center, and was occupied by over 30,000 military personnel in 1944. After the end of the war, the naval air station operated on the island, with resident populations up to 6,000, until its closure in 1997. As a result of this military history, the town has extensive infrastructure, including two large paved airport runways and multiple deep-water ship berthing piers (Figure 3). After the base closure, most property and facilities within the town, as well as much of the northern part of the island, were transferred from the United States

government to Aleut Corporation, an Alaska Native Regional Corporation (Sepez *et al.* 2005). Lands in the southern portion of Adak Island are part of the Alaska Maritime National Wildlife Refuge, managed by the U.S. Fish and Wildlife Service.

Event history and records

Tsunamis have long been a known hazard in the Aleutians, including Adak. There is evidence of the destruction of an Aleut village on the west side of the island 3000 years B.P. (Fraser *et al.* 1959) The risk of tsunamis may have been a factor in the location of early indigenous settlements on the more protected Bering Sea side of the islands, instead of on the open Pacific Ocean coast (McCartney *et al.* 1999).

The NOAA National Ocean Service (NOS) tide gauge at Adak was established in August 1943, and has recorded most significant Pacific basin tsunamis since that time. The tide station is the westernmost station operated by NOS in Alaska. The West Coast/Alaska Tsunami Warning Center (WCATWC) operates two tide stations further west, at Amchitka and Shemya. Sweeper Cove, Adak's main harbor, is protected by a breakwater extending from the north side of the harbor. The tide station is located at 176.6347°W 51.8162°N, near the midpoint of the harbor's Pier 3 (Figure 4). Water depths near the tide gauge are approximately 12 m below mean high water.

Table 1 summarizes the historic events used for testing the model at Adak. Details of events particularly notable to Adak's tsunami history are described here. Adak was the first coastal tide station to record waves for several major tsunamis occurring near the Andreanof Islands, illustrating its value for forecasting purposes.

The first major event after the NOS tide gauge's installation was the April 1, 1946 Unimak tsunami (M_w 8.5). The surviving image of the tide gauge marigram for this event is illegible, but Lander (1996) reports a small (4 inch maximum amplitude) signal at Adak.

The March 9, 1957 Andreanof earthquake (M_w 8.6) is the largest to be recorded seismically along the subduction zone immediately adjacent to the Andreanof Islands (Johnson *et al.* 1994), and is the largest tsunami event recorded at Adak in terms of wave amplitude. A 1.91 m amplitude wave (12.5 feet, peak-to-trough) hit Adak's Sweeper Cove, causing substantial damage. Great Sitkin Island's Sand Bay, 37 km east northeast of Adak across Sitkin Sound, saw a 4 m amplitude wave (Lander 1996). No tide gauge record from Adak survives for this event, presumably because the tide gauge equipment was destroyed by waves.

The May 22, 1960 Chile earthquake (M_w 9.2) and tsunami caused extensive damage in the Pacific Basin; while it caused no substantial damage in Alaska, it was recorded more strongly in the Aleutian Islands than anywhere else in the state (Lander 1996). The source model used for testing in this study is derived from the source parameters developed by Kanamori and Cipar (1974). The original marigram was digitized for this study from the archives of the National Geophysical Data Center.

The March 28, 1964 Gulf of Alaska earthquake (M_w 9.2) and tsunami caused extensive damage in south-central Alaska, as well as elsewhere in the Pacific, but produced a modest 0.3 m (amplitude) wave at

Adak, causing no recorded damage (Lander 1996). The source model used for testing has been previously used by other hazard assessment studies around the Pacific (Tang *et al.* 2006).

The May 7, 1986 Andreanof Islands earthquake (M_w 8.0) was the largest earthquake along the subduction zone adjacent to Adak to occur since 1957. It produced a 0.88 m amplitude wave at Adak, arriving with 18 min after the event, making this the closest event to Adak to be recorded by the tide gauge (Lander 1996). This event thus provides a valuable case for testing the model's performance with near-field events. The source model used for testing this event was derived from the source parameters developed by Hwang and Kanamori (1986), the same source parameters used for some previous modeling work of this event at Adak (Kowalik *et al.* 1991).

Just over ten years after the 1986 event, the June 10, 1996 Andreanof earthquake (M_w 7.9) along the subduction zone immediately adjacent to Adak produced a tsunami recorded throughout the Pacific, including at deep-ocean bottom-pressure recorders deployed in the Aleutians and along the United States West Coast (Eble *et al.* 1997). Adak was the first onshore tide gauge to record the tsunami waves, with a non-destructive 0.5 m wave arriving approximately ten minutes after the earthquake.

Of the major Pacific basin tsunamis to occur since 2000, none have produced substantial waves at Adak. The November 15, 2006 Kuril earthquake (M_w 8.3) and tsunami produced 20 cm amplitude, and the February 27, 2010 Chile earthquake (M_w 8.8) produced 38 cm amplitude waves, the largest at Adak since 1996.

Bathymetric grid and model setup

As described above, forecast model creation required the development of two sets of three nested grids: a higher-resolution reference model, and a lower-resolution forecast model. Both sets of grids were derived from two source datasets developed by the National Geophysical Data Center (NGDC).

A one-arc-second (approximately 30 m) cell size grid covering Adak and nearby islands (Carignan *et al.* 2009) provided source material for the higher-resolution (B and C) grids. This combined bathymetric/topographic grid was developed by NGDC under contract from NCTR specifically for tsunami modeling. The bathymetric surface is derived primarily from National Ocean Service (NOS) surveys, except in deep-water areas where some research multibeam survey results were available, and some limited areas where soundings from electronic charts were incorporated. Topographic data was derived primarily from the NASA Shuttle Radar Topography Mission (SRTM) global dataset, enhanced in several areas with individual data points from other data sources. Vertical elevations in the grid were in meters above/below mean high water (MHW); this is thus the vertical datum at which the model runs.

Outside of the area covered by the Adak grid, the model grids were derived from NGDC's ETOPO1 global dataset (Amante *et al.* 2009). Bathymetry in the Adak area in this dataset is primarily estimated from satellite altimetry readings. This dataset was resampled to the resolution of the outermost (A) model grids and mosaiced with the Adak dataset.

Three reference model grids and three forecast model grids were created by cropping and resampling these source grids (Figure 5). Table 2 contains the details of the model grid extents, grid node spacing, and model settings.

Broadly, the outermost (A) grid's role is to model wave dynamics as the tsunami transitions from propagation in the deep open ocean into the shallower Andreanof region. The southern extent of the high-resolution reference model was set to include the adjacent Aleutian Trench, the entire Andreanof Islands archipelago, and the wide adjacent Amchitka and Amutka Passes. Experimentation with the model extents showed that excluding the deep water of the Aleutian Trench from the grid had little impact on modeled waves at Adak, indicating that wave dynamics in the deep water are well-described by the pre-computed propagation database. Thus the southern extent of the forecast model could be set substantially further north. This change reduces the number of nodes in the forecast grid, but also reduces the maximum depth in the grid from 7725 m (reference model) to 6035 m (forecast model), allowing a longer model timestep that still satisfies the CFL condition.

The middle (B) grid covers the island of Adak and several smaller outlying islands, modeling wave dynamics as the tsunami travels along the coastline and through the several narrow passes between islands. The complexity of these passages constrained the development of the forecast grid, The innermost (C) grid covers the Adak harbor area. It must be of sufficient resolution to provide useful flooding forecasts, as well as to accurately model wave dynamics at the tide gauge. Evaluation of several candidate forecast model C grids showed that only the inner parts of Kuluk Bay, and Sweeper Cove itself, had a substantial impact on wave dynamics at the tide gauge in the inner harbor. Thus the forecast model C grid has a substantially smaller extent than the reference grid.

To further optimize the number of grid nodes and timestep requirements, grid node spacing varies within each forecast model grid (Figure 6). Selectively using a larger node spacing over the deepest regions of the grids in the A and C grids allowed a somewhat longer model timestep that still satisfied the CFL condition for stability. It also reduced the total number of nodes in each grid, reducing the computational intensity of the model. The B grid used a closer grid spacing to cover Kagalaska Strait, a narrow passageway difficult to correctly model at typical B grid resolutions that was nevertheless expected to be an important opening for tsunami waves into the Adak harbor area.

Model validation and testing

The model testing process is intended to ensure that the model meets two major requirements that make it usable as part of an operational forecast system:

1. The model must accurately predict the actual wave dynamics at the location.
2. The model must be numerically stable for all plausible event source scenarios.

To validate model accuracy, we compare forecast model results with reference model results recorded tide gauge records for several. To validate numerical stability, we use a suite of large earthquake source scenarios, as well as a very small (no-wave) scenario.

Historical event validation

As discussed above, Adak has a substantial tsunami history, with several tide gauge records available. To test the accuracy with which the model reproduces actual wave dynamics, we compare results produced by the reference and forecast models at the Adak tide gauge location with the tide gauge record of the event.

Figures 7 – 18 summarize these comparisons, showing maximum amplitudes in the C grid for the reference and forecast models, and a timeseries at the tide gauge location for each model and the tide gauge record where available. Tide gauge records were processed by removing the output of a low-pass Butterworth filter from the raw tide signal to remove the tide signal. For comparison purposes, the maximum amplitude diagrams are plotted with the same scale and extent, but the forecast model grid covers a smaller area.

In general, comparison is good between the model results and the tide gauges. Wave arrival time comparisons are generally very good. For later waves, several hours after the start of the model run, the forecast model sometimes reports somewhat smaller amplitudes than the reference model. For relatively small events (recorded maximum amplitudes < 15 cm), the narrow passages between islands lead to somewhat under-predicting the actual tide gauge record.

Stability testing

To evaluate the stability of the model under a wide range of conditions, it was tested using a suite of extremely large and small hypothetical source scenarios. Nineteen large source scenarios equivalent to a M_w 9.4 earthquake were used. These sources were constructed from combination of twenty unit sources (a region of 1000 x 100 km) with a slip (scaling factor) of 30 m. These sources were located along all of the Pacific Ocean subduction zones covered by NOAA's propagation database. Figure 19 shows the timeseries results at Adak.

The largest amplitude scenarios (acsz_16_25 and acsz_6_15) both result from earthquakes along the Aleutian subduction zone immediately adjacent to Adak. These produce extremely large waves, up to 10 m maximum amplitude, and extensive inundation in the Adak area, but examination of the model output shows that the model remained stable, and continued to produce physically plausible results.

In addition to stability with extremely large waves, the model was also validated to produce correct results with very small input boundary condition waves. In this situation, the model is expected to also output little or no waves; a numerically unstable model might produce ringing or increasing amplitudes in this situation. The Adak forecast model was tested in this "no-wave" case by using an equivalent of a M7.0 earthquake along the East Philippines subduction zone (0.18 m slip on source epsza0). In the Adak area, this scenario produces waves less than 0.2 cm amplitude in the propagation data. Resulting waves in the forecast model grids remained under 0.6 cm.

Conclusion

A tsunami forecast model covering the Adak, Alaska area has been created for inclusion into NOAA's operational tsunami forecast system. This model is capable of forecasting wave amplitudes, arrival times, and flooding at Adak for tsunami events throughout the Pacific Ocean. The model grids are derived from a compilation of the best available bathymetry for the region. The model has been validated against historical data and tested for stability against very large and small input source scenarios.

The result is a reliable component of the growing forecast system. It expands the forecast system coverage in the Aleutian Islands; in a real-time forecast situation, model results at this remote location will be valuable both for protecting life and property in Adak, but also for model-data comparisons to improve forecasts in other parts of the Pacific.

Acknowledgements

Kelly Stroker of the National Geophysical Data Center provided tide gauge records for older historical events.

References

Amante, C. and B.W. Eakins (2009): ETOPO1 1 Arc-Minute Global Relief Model: Procedures, Data Sources and Analysis. NOAA Tech Memo NESDIS NGDC-24**:** 19 pp.

Carignan, K.S., L.A. Taylor, B.W. Eakins, R.R. Warnken, P.R. Medley and E. Lim (2009): Digital elevation model of Adak, Alaska: Procedures, data sources, and analysis. NOAA Tech. Memo. NESDIS NGDC-31. NOAA National Geophysical Data Center, Boulder, CO.

Eble, M.C., J. Newman, J. Wendland, B. Kilonsky, D. Luther, Y. Yanioka, M. Okada and F.I. González (1997): The 10 June 1996 Andreanof tsunami database. NOAA Tech. Memo. ERL PMEL-64. NOAA Pacific Marine Environmental Laboratory, Seattle, WA**:** 33 pp.

Fraser, G.D. and G.L. Snyder (1959): Geology of Southern Adak Island and Kagalaska Island, Alaska. USGS Bulletin 1028-M.

Gica, E., M. Spillane, V.V. Titov, C.D. Chamberlin and J. Newman (2008): Development of the forecast propagation database for NOAA's Short-term Inundation Forecast for Tsunamis (SIFT). NOAA Tech Memo OAR PMEL-139. NOAA Pacific Marine Environmental Laboratory, Seattle, WA**:** 89 pp.

Hwang, L.J. and H. Kanamori (1986): Source parameters of the May 7, 1986 Andreanof Islands earthquake. *Geophys. Res. Lett.* 13(13): 1426-1429.

Johnson, J.M., Y. Tanioka, L.J. Ruff, K. Satake, H. Kanamori and L.R. Sykes (1994): The 1957 great Aleutian earthquake. *Pure and Applied Geophysics* 142(1).

Kanamori, H. and J.J. Cipar (1974): Focal process of the great Chilean earthquake, May 22, 1960. *Physics of The Earth and Planetary Interiors* 9: 128-136.

Kowalik, Z. and P.W. Whitmore (1991): An investigation of two tsunamis recorded at Adak, Alaska. *Science of Tsunami Hazards* 9: 67-83.

Lander, J.F. (1996): Tsunamis affecting Alaska, 1737-1996. NGDC Key to Geophysical Research. NOAA National Geophysical Data Center, Boulder, CO.

McCartney, A.P. and D.W. Veltre (1999): Aleutian Island prehistory: living in insular extremes. *World Archaeology* 30(3): 503-515.

Sepez, J.A., B.D. Tilt, C.L. Package, H.M. Lazarus and I. Vaccaro (2005): Community profiles for North Pacific fisheries - Alaska. NOAA Tech. Memo. NMFS-AFSC-160**:** 552p.

Synolakis, C.E., E.N. Bernard, V.V. Titov, U. Kânoğlu and F.I. González (2008): Validation and verification of tsunami numerical models. *Pure and Applied Geophysics* 165(11-12): 2197–222.

Tang, L., C.D. Chamberlin, E. Tolkova, M. Spillane, V.V. Titov, E.N. Bernard and H.O. Mofjeld (2006): Assessment of potential tsunami impact for Pearl Harbor, Hawaii. NOAA Tech Memo OAR-PMEL-131. NOAA Pacific Marine Environmental Laboratory, Seattle, WA**:** 36 pp.

Tang, L., V.V. Titov and C.D. Chamberlin (2009): Development, testing, and applications of site-specific tsunami inundation models for real-time forecasting. *J. Geophys. Res.-Oceans* 114: 22.

Tang, L., V.V. Titov, Y. Wei, M. H.O., M. Spillane, D. Arcas, E.N. Bernard, C. Chamberlin, E. Gica and J. Newman (2008): Tsunami forecast analysis for the May 2006 Tonga tsunami. *J. Geophys. Res.* 113.

Titov, V.V. (2009): Tsunami forecasting. *The Sea, Volume 15: Tsunamis*. E. N. Bernard and A. R. Robinson. Cambridge MA and London, England, Harvard University Press**:** 371-400.

Titov, V.V. and F.I. González (1997): Implementation and testing of the Method of Splitting Tsunami (MOST) model NOAA Tech Memo ERL PMEL-112. NOAA Pacific Marine Environmental Laboratory, Seattle, WA**:** 11 pp.

Titov, V.V., F.I. González, E.N. Bernard, M.C. Eble, H.O. Mofjeld, J. Newman and A.J. Venturato (2005): Real-time tsunami forecasting: Challenges and solutions. *Natural Hazards* 35(1): 41-58.

Wei, Y., E.N. Bernard, L. Tang, V.V. Titov, C. Moore, M. Spillane, M. Hopkins and U. Kânoğlu (2008): Real-time experimental forecast of the Peruvian tsunami of August 2007 for U.S. coastlines. *Geophys. Res. Lett.* 35(L04609).

Figures

Tables

Earthquake / Seismic				Model		
Event	USGS Date Time (UTC) Epicenter	CMT Date Time (UTC) Centroid	Magnitude Mw	Tsunami Magnitude[1]	Subduction Zone	Tsunami Source
1946 Unimak	01 Apr 12:28:56 52.75ºN 163.50ºW	01 Apr 12:28:56 53.32ºN 163.19ºW	[2]8.5	8.5	Aleutian-Alaska-Cascadia (ACSZ)	7.5 × b23 + 19.7 × b24 + 3.7 × b25
1957 Andreanov	09 Mar 14:22:31 51.56ºN 175.39ºW	09 Mar 14:22:31.9 51.292ºN 175.629ºW	[3]8.6	8.7	Aleutian-Alaska-Cascadia (ACSZ)	31.4 × a15 + 10.6 × a16 + 12.2 × a17
1960 Chile	22 May 19:11:14 [3]38.29ºS 73.05ºW	22 May 19:11:14 38.50ºS 74.50ºW	[4]9.5		Central-South America (CSSZ)	Kanamori and Ciper (1974)
1964 Alaska	28 Mar 03:36:00 [3]61.02ºN 147.65ºW	28 Mar 03:36:14 61.10ºN 147.50ºW	[3]9.2	9.0	Aleutian-Alaska-Cascadia (ACSZ)	Tang *et al.* (2006)
1986 Andreanov	07 May 22:47:10 [3]51.52ºN 174.78ºW	07 May 22:47:10 [3]51.52ºN 174.78ºW	[3]8.0		Aleutian-Alaska-Cascadia (ACSZ)	Hwang and Kanamori (1986)
1994 East Kuril	04 Oct 13:22:58 43.73ºN 147.321ºE	04 Oct 13:23:28.5 43.60ºN 147.63ºE	[5]8.3	8.1	Kamchatka-Kuril-Japan-Izu-Mariana-Yap (KISZ)	9.0 × a20
1996 Andreanov	10 Jun 04:03:35 51.56ºN 175.39ºW	10 Jun 04:04:03.4 51.10ºN 177.410ºW	[5]7.9	7.8	Aleutian-Alaska-Cascadia (ACSZ)	2.40 × a15 + 0.80 × b16
2001 Peru	23 Jun 20:33:14 16.265ºS 73.641ºW	23 Jun 20:34:23.3 17.28ºS 72.71ºW	[5]8.4	8.2	Central-South America (CSSZ)	5.7 × a15 + 2.9 × b16 + 1.98 × a16
2003 Rat Island	17 Nov 06:43:07 51.13ºN 178.74ºE	17 Nov 06:43:31.0 51.14ºN 177.86ºE	[5]7.7	7.8	Aleutian-Alaska-Cascadia (ACSZ)	[6]2.81 × b11
2006 Tonga	03 May 15:26:39 20.13ºS 174.161ºW	03 May 15:27:03.7 20.39ºS 173.47ºW	[5]8.0	8.0	New Zealand-Kermadec-Tonga (NTSZ)	6.6 × b29
2006 Kuril	15 Nov 11:14:16 46.607ºN 153.230ºE	15 Nov 11:15:08 46.71ºN 154.33ºE	[5]8.3	8.1	Kamchatka-Kuril-Japan-Izu-Mariana-Yap (KISZ)	[6]4 × a12 + 0.5 × b12 + 2 × a13 + 1.5 × b13
2007 Solomon	01 Apr 20:39:56 8.481ºS 156.978ºE	01 Apr 20:40:38.9 7.76ºS 156.34ºE	[3]8.1	8.2	New Britain-Solomons-Vanuatu (NVSZ)	12.0 × b10
2009 Samoa	29 Sep 17:48:10 15.509ºS 172.034ºW	29 Sep 17:48:26.8 15.13ºS 171.97ºW	[5]8.1	8.1	New Zealand-Kermadec-Tonga (NTSZ)	[6]3.96 × a34 + 3.96 × b34
2010 Chile	27 Feb 06:34:14 35.909ºS 72.733ºW	27 Feb 06:35:15.4 35.95ºS 73.15ºW	[5]8.8	8.8	Central-South America (CSSZ)	[6]a88 × 17.24 + a90 × 8.82 + b88 × 11.86 + b89 × 18.39 + b90 × 16.75 + z88 × 20.78 + z90 × 7.06

[1] Preliminary source – derived from source and deep-ocean observations
[2] López and Okal (2006)
[3] United States Geological Survey (USGS)

		Reference Model				Forecast Model			
Grid	**Region**	**Coverage** Lat. [ºN] Lon. [ºW]	**Cell size** Lat. Lon	**Nodes** Lat. Lon.	**Time Step** [sec]	**Coverage** Lat. [ºN] Lon. [ºW]	**Cell size** Lat. Lon.	**Nodes** Lat. Lon.	**Time Step** [sec]
A	Central Aleutians	50.2 - 53.1 179.25 - 189.25	36” 24”	436 1001	1.8	50.95 - 52.60 180.5 - 187.1	1.1’ 1.55’ [1]	92 255	6.4
B	Adak Island	51.475 - 52.075 182.85 - 184.10	6” 9”	361 501	0.9	52.07 - 51.50 182.85 - 184.1	13.33” 18.96” [2]	154 238	1.6
C	Adak harbor	51.81 - 51.96 183.60 - 183.33	1.0” 1.2”	541 811	0.45	51.818 - 51.93 183.46 - 183.335	2.0” 3.15” [3]	203 149	1.6
Minimum offshore depth [m]				10.0 m				2.0	
Water depth for dry land [m]				0.1				0.1	
Friction coefficient [n^2]				0.0009				0.0009	
CPU time for 4-hr simulation				1.4 hours					

Computations were performed on a single Intel Xeon processor at 3.6 GHz, Dell PowerEdge 1850.

[1] These are average cell sizes. Cell sizes in the forecast model A grid vary between 1.5’ – 1.75’ in the longitude direction, and 1’ – 1.5’ in the latitude direction. See Figure 6 for details.

[2] Cell sizes in the forecast model B grid vary between 12” – 20” in the longitude direction. Cell sizes are constant in the latitude direction.

[3] Cell sizes in the forecast model C grid vary between 3” – 4” in the longitude direction. Cell sizes are constant in the latitude direction.

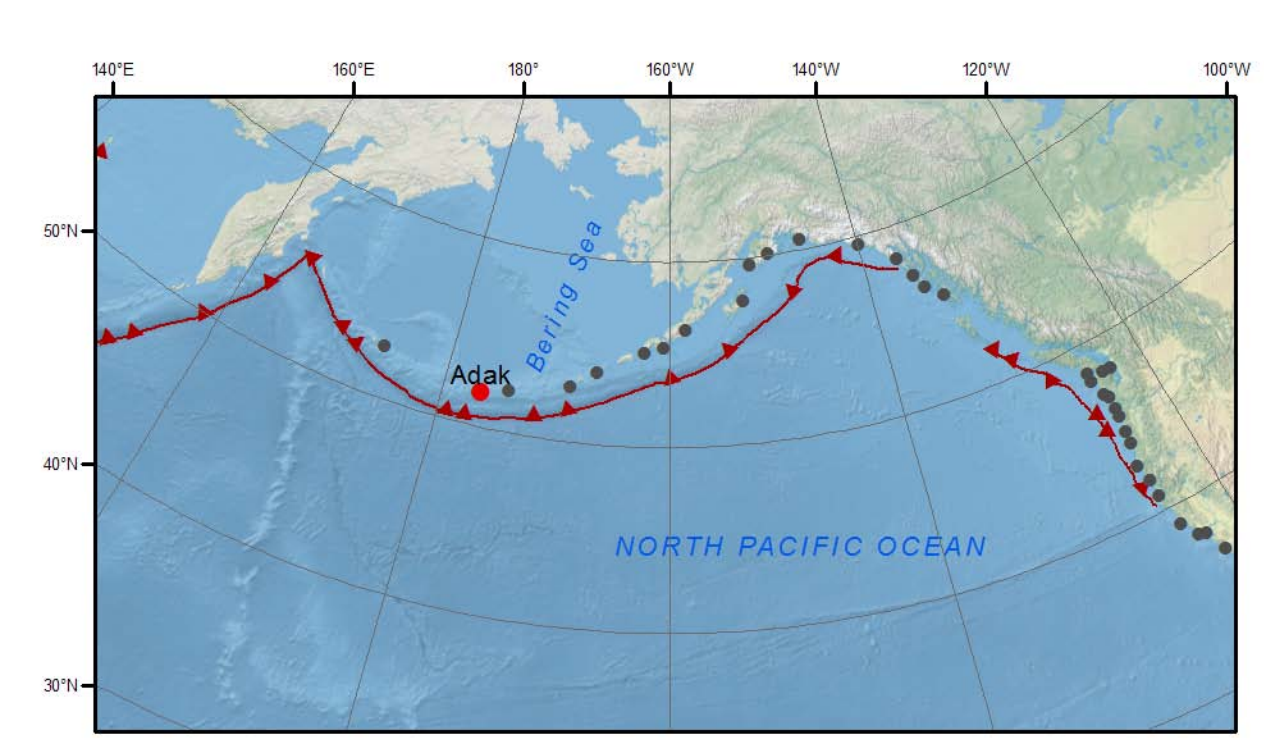
140°E
160°E
180°
160°W
140°W
120°W
100°W
50°N
40°N
30°N
Bering Sea
Adak
NORTH PACIFIC OCEAN

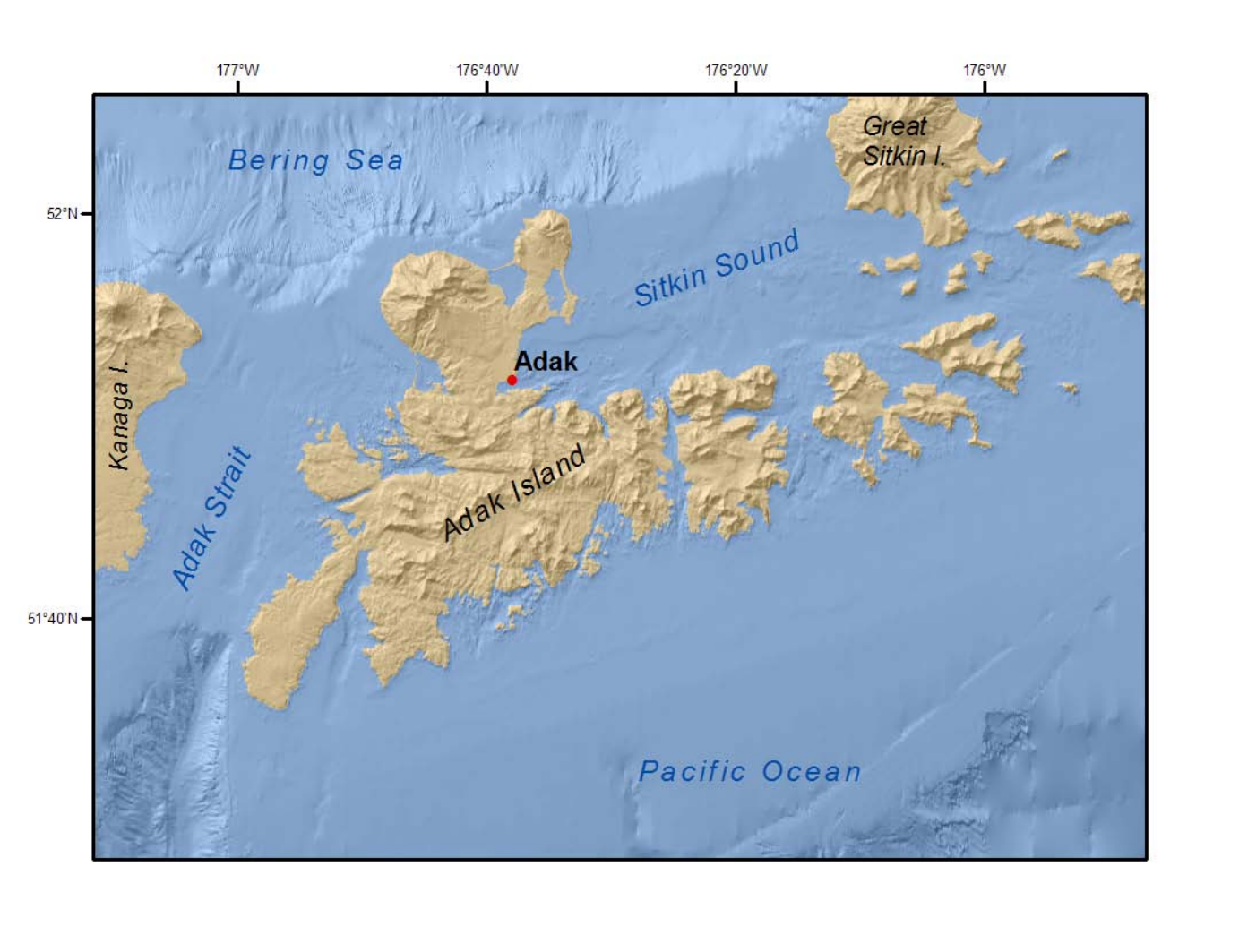
177°W
176°40'W
176°20'W
176°W
52°N
51°40'N
Bering Sea
Great
Sitkin I.
Sitkin Sound
Adak
Kanaga I.
Adak Strait
Adak Island
Pacific Ocean

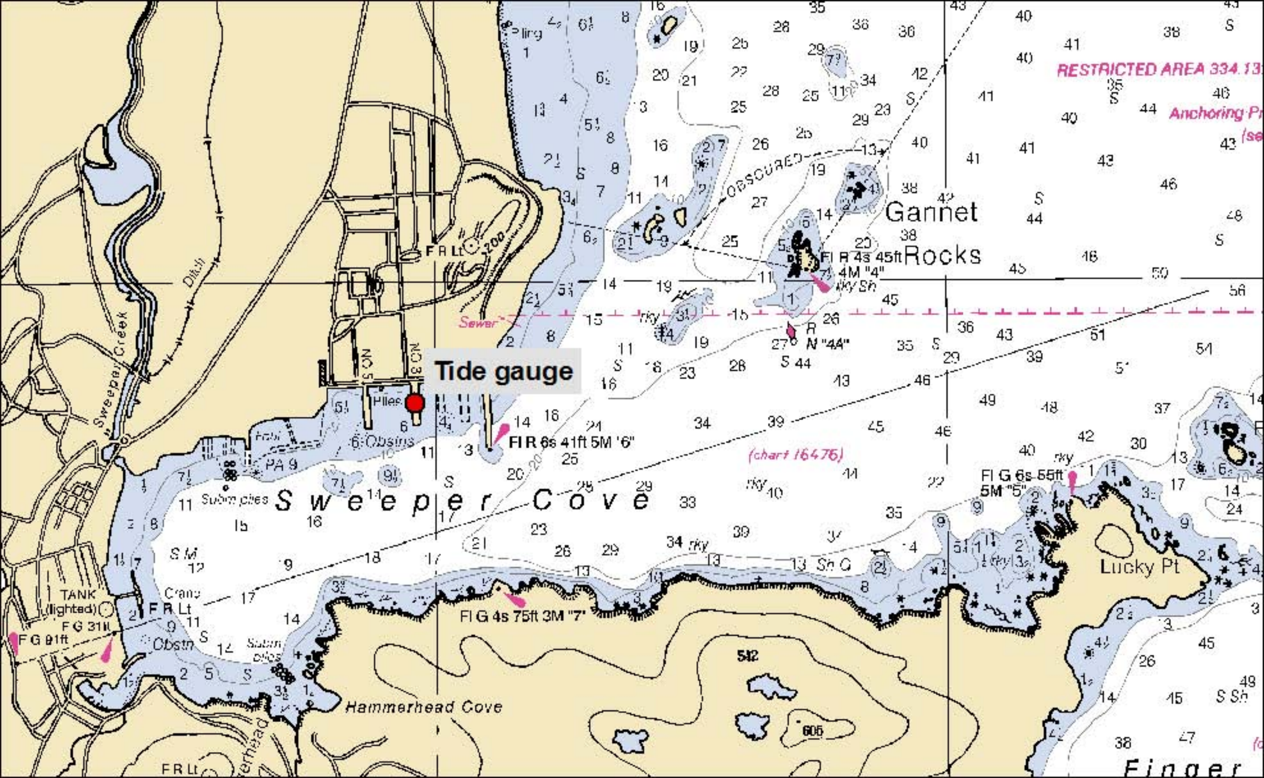
Tide gauge
Gannet
Rocks
Sweeper Cove
Hammerhead Cove
Lucky Pt
Sweeper Creek
RESTRICTED AREA 334.13
OBSCURED
Fl R 4s 45ft 4M "4"
Fl R 6s 41ft 5M "6"
Fl G 6s 55ft 5M "5"
Fl G 4s 75ft 3M "7"
F R Lt
F G 31ft
F G 91ft
TANK (lighted)
Sewer
Piles
Obstns
Subm piles
(chart 16476)
R N "4A"

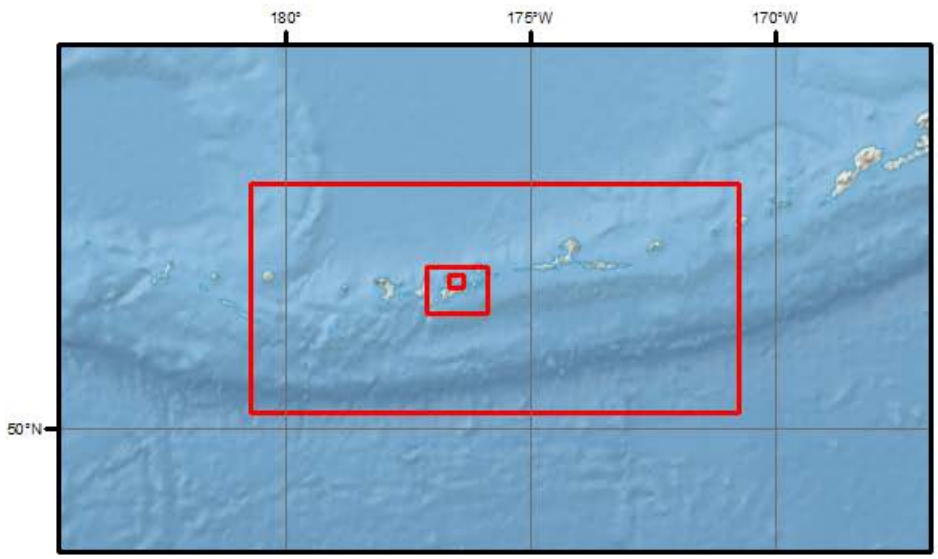
180°
175°W
170°W
50°N

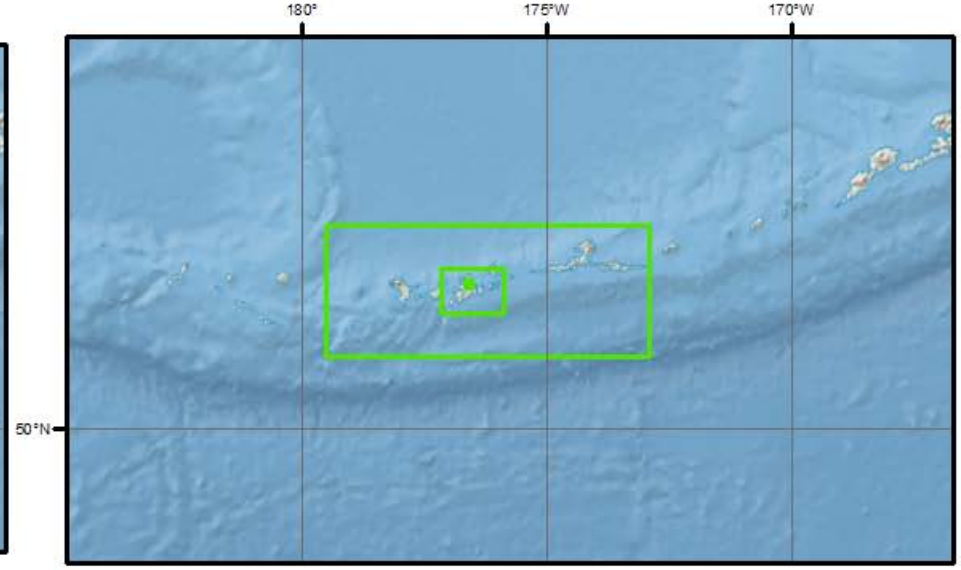
180°
175°W
170°W
50°N

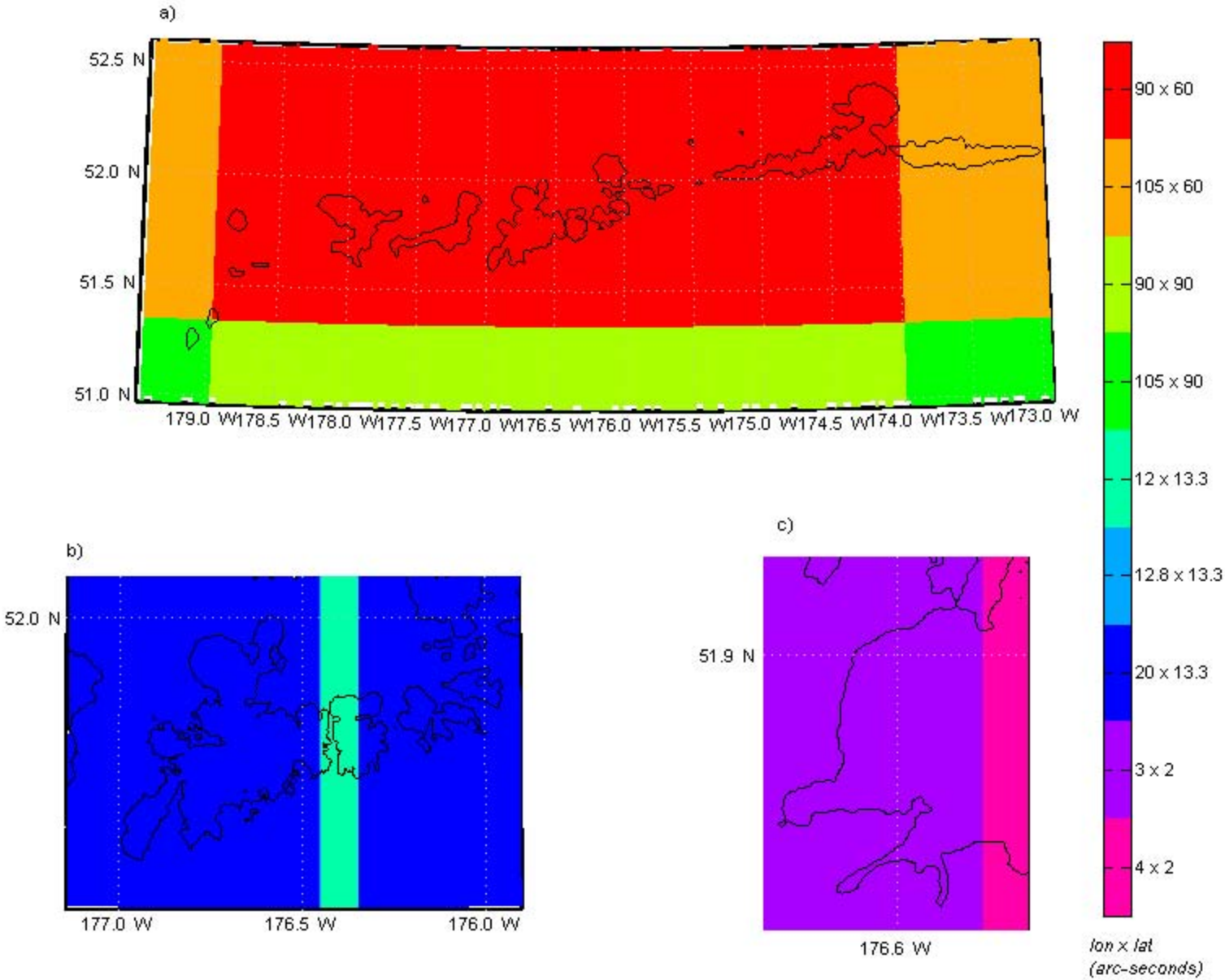
a)
52.5 N
52.0 N
51.5 N
51.0 N
179.0 W
178.5 W
178.0 W
177.5 W
177.0 W
176.5 W
176.0 W
175.5 W
175.0 W
174.5 W
174.0 W
173.5 W
173.0 W
b)
52.0 N
177.0 W
176.5 W
176.0 W
c)
51.9 N
176.6 W
90 x 60
105 x 60
90 x 90
105 x 90
12 x 13.3
12.8 x 13.3
20 x 13.3
3 x 2
4 x 2
lon x lat
(arc-seconds)

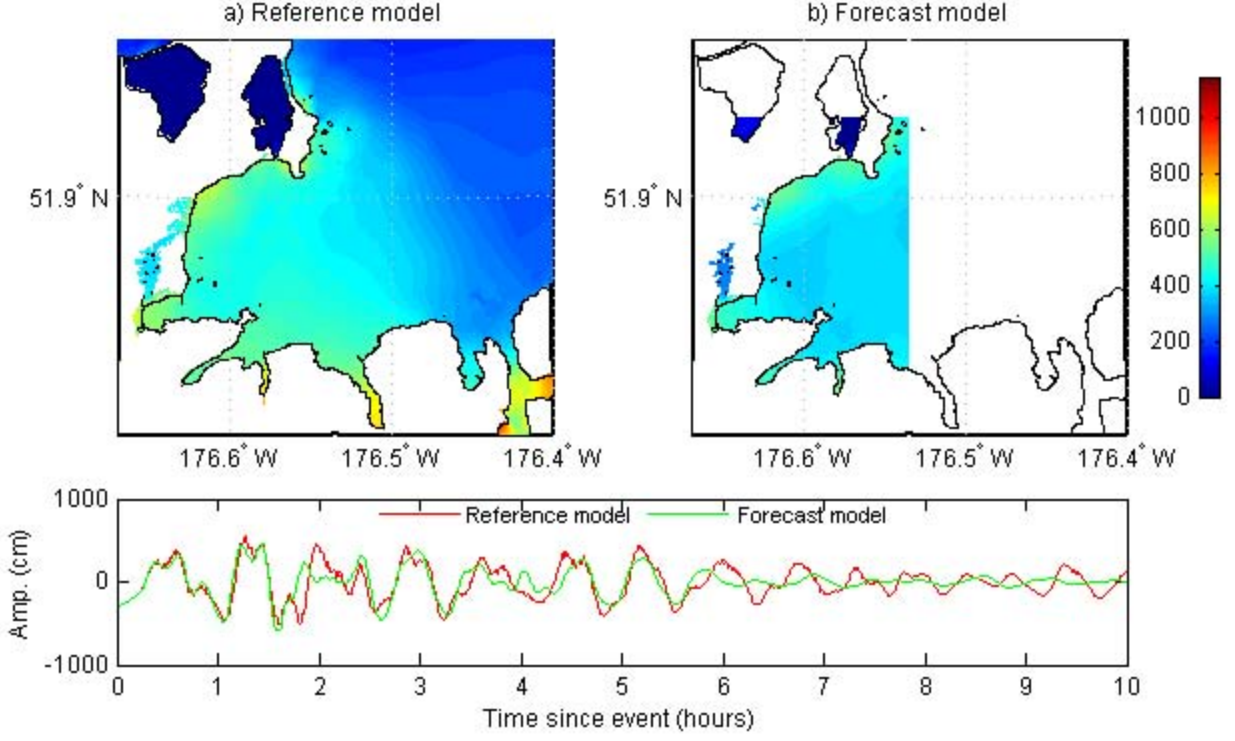
a) Reference model
b) Forecast model
51.9° N
51.9° N
176.6° W
176.5° W
176.4° W
176.6° W
176.5° W
176.4° W
1000
800
600
400
200
0
Reference model
Forecast model
Amp. (cm)
1000
0
-1000
0
1
2
3
4
5
6
7
8
9
10
Time since event (hours)

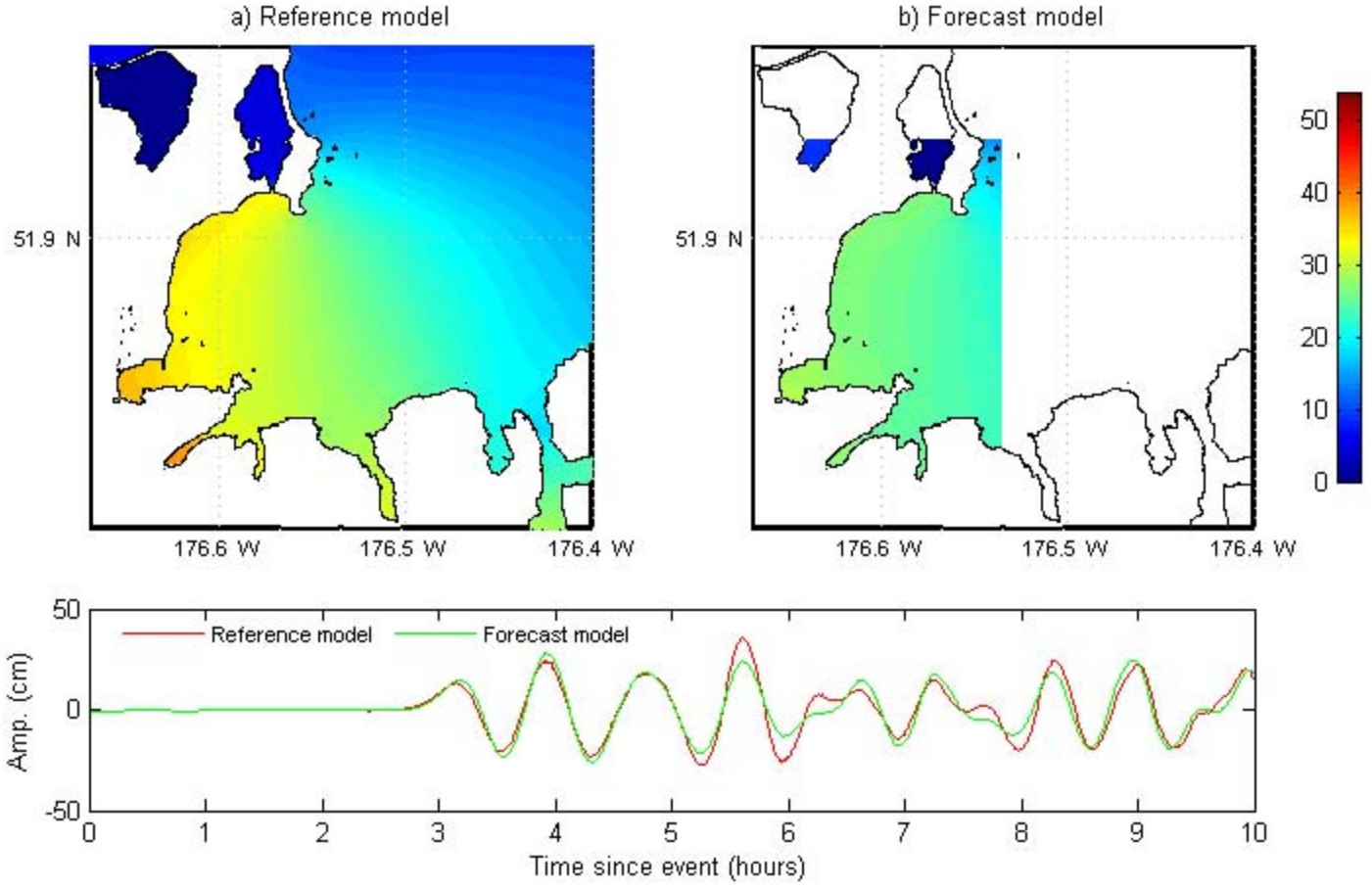
a) Reference model
b) Forecast model
51.9 N
51.9 N
176.6 W
176.5 W
176.4 W
176.6 W
176.5 W
176.4 W
50
40
30
20
10
0
Reference model
Forecast model
Amp. (cm)
50
0
-50
0
1
2
3
4
5
6
7
8
9
10
Time since event (hours)

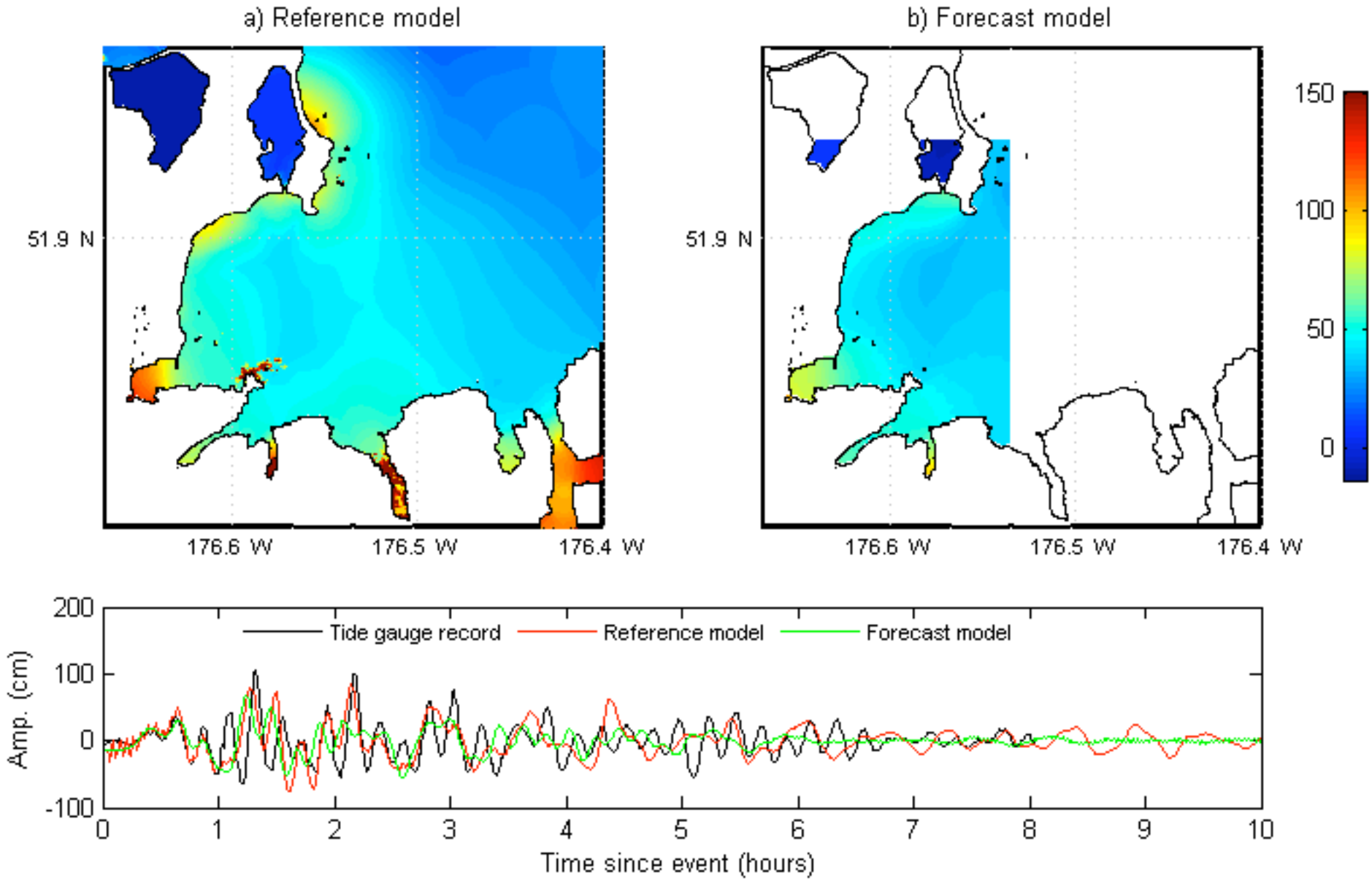
a) Reference model
b) Forecast model
51.9 N
176.6 W
176.5 W
176.4 W
150
100
50
0
Tide gauge record
Reference model
Forecast model
Amp. (cm)
200
100
0
-100
0
1
2
3
4
5
6
7
8
9
10
Time since event (hours)

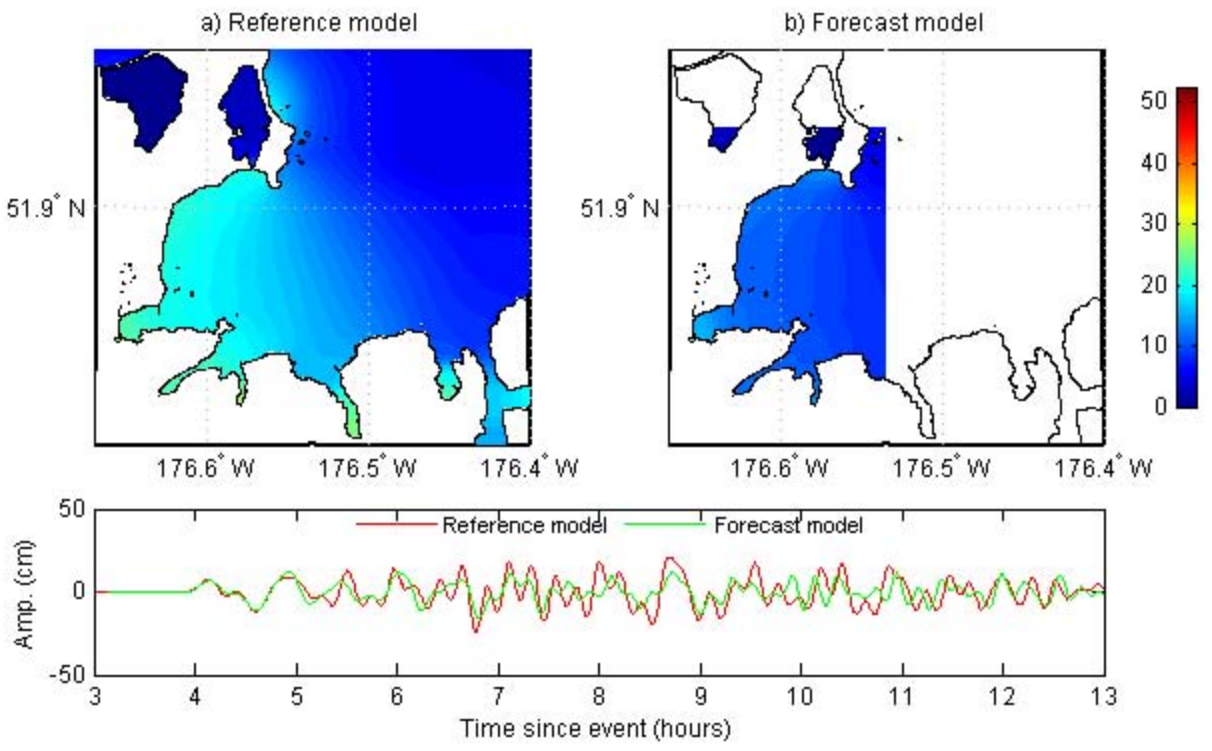
a) Reference model
b) Forecast model
51.9° N
51.9° N
176.6° W
176.5° W
176.4° W
176.6° W
176.5° W
176.4° W
50
40
30
20
10
0
Reference model
Forecast model
Amp. (cm)
50
0
-50
3
4
5
6
7
8
9
10
11
12
13
Time since event (hours)

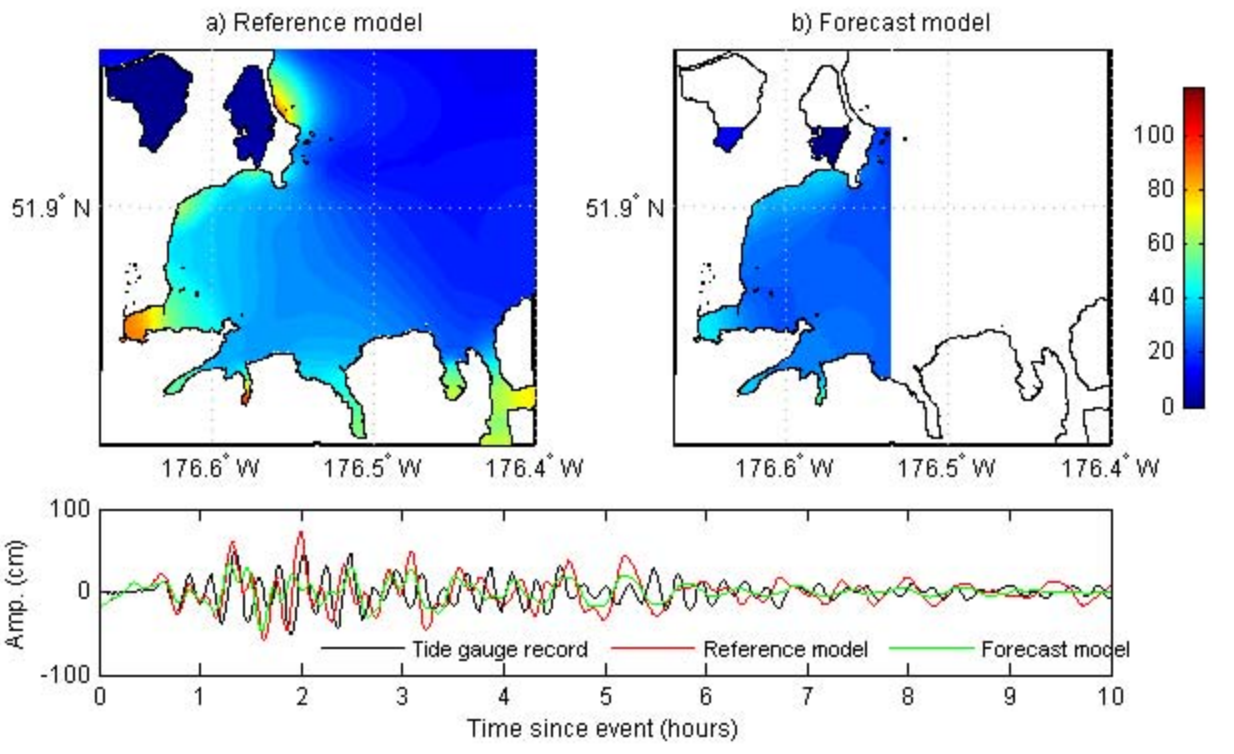
a) Reference model
b) Forecast model
51.9° N
51.9° N
176.6° W
176.5° W
176.4° W
176.6° W
176.5° W
176.4° W
100
80
60
40
20
0
100
0
-100
Amp. (cm)
Tide gauge record
Reference model
Forecast model
0
1
2
3
4
5
6
7
8
9
10
Time since event (hours)

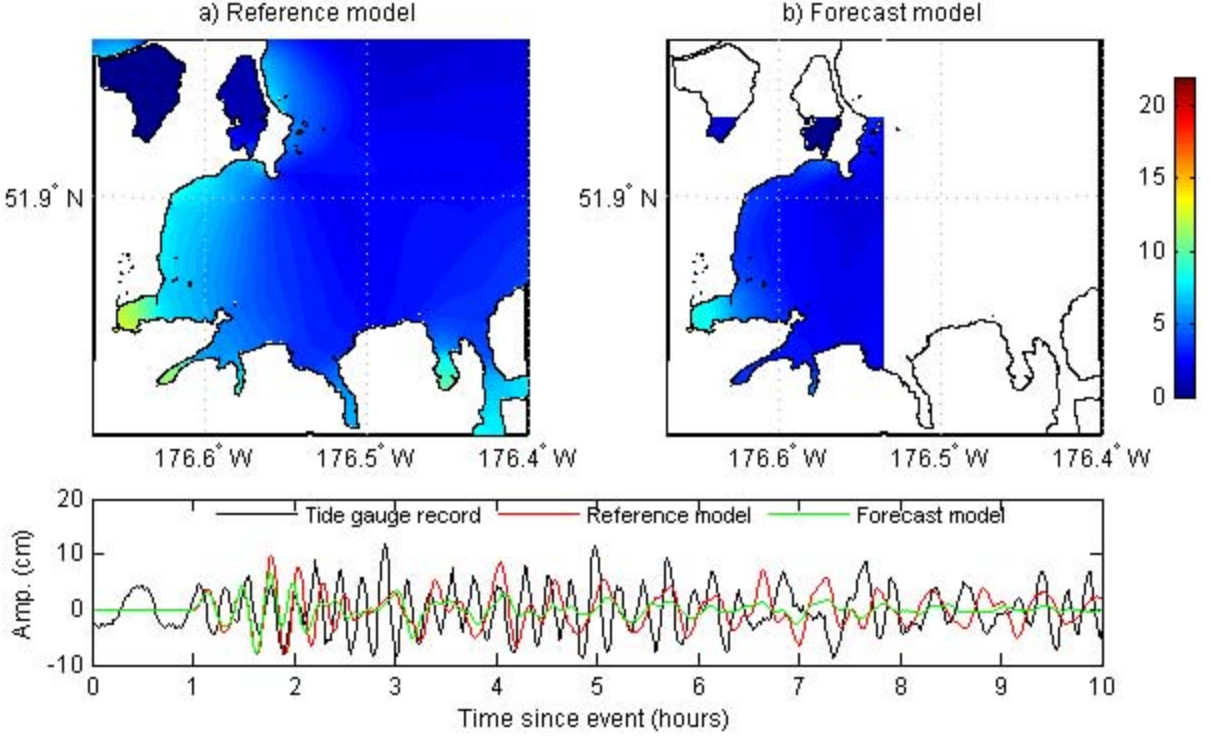
a) Reference model
b) Forecast model
51.9° N
51.9° N
176.6° W
176.5° W
176.4° W
176.6° W
176.5° W
176.4° W
20
15
10
5
0
Tide gauge record
Reference model
Forecast model
Amp. (cm)
20
10
0
-10
0
1
2
3
4
5
6
7
8
9
10
Time since event (hours)

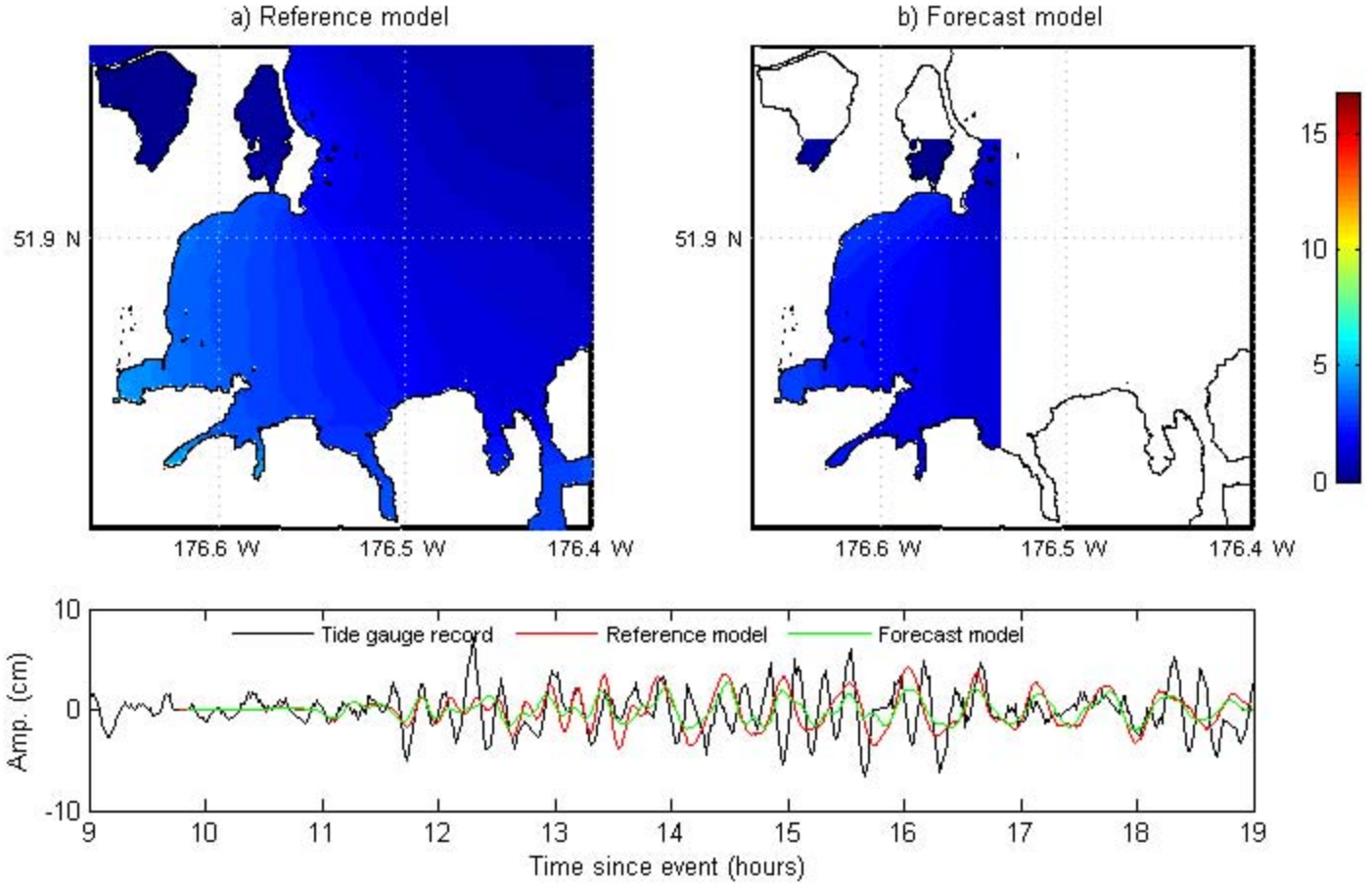
a) Reference model
b) Forecast model
51.9 N
51.9 N
176.6 W
176.5 W
176.4 W
176.6 W
176.5 W
176.4 W
15
10
5
0
Tide gauge record
Reference model
Forecast model
Amp. (cm)
10
0
-10
9
10
11
12
13
14
15
16
17
18
19
Time since event (hours)

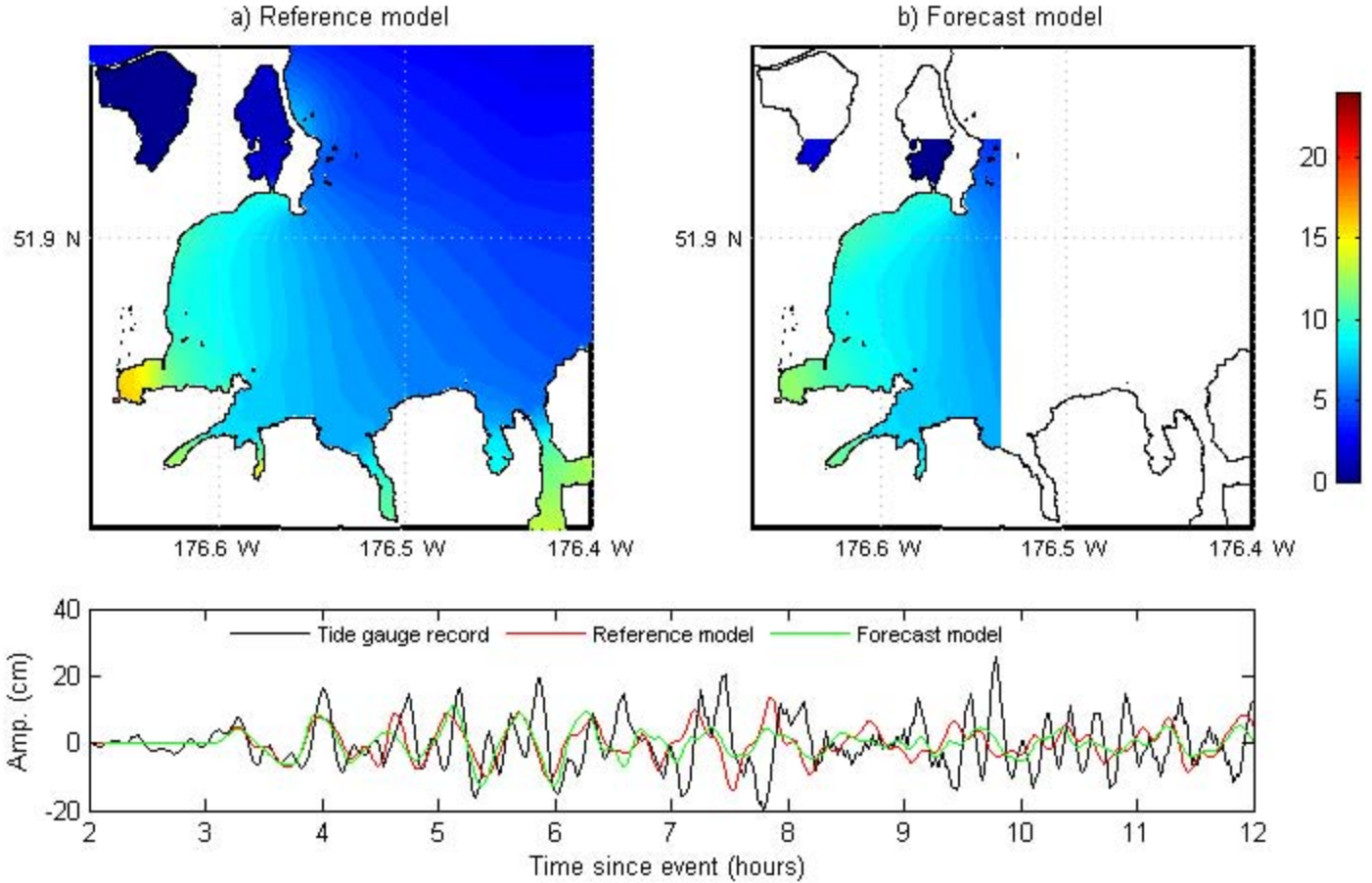
a) Reference model
b) Forecast model
51.9 N
51.9 N
176.6 W
176.5 W
176.4 W
176.6 W
176.5 W
176.4 W
20
15
10
5
0
Tide gauge record
Reference model
Forecast model
Amp. (cm)
40
20
0
-20
2
3
4
5
6
7
8
9
10
11
12
Time since event (hours)

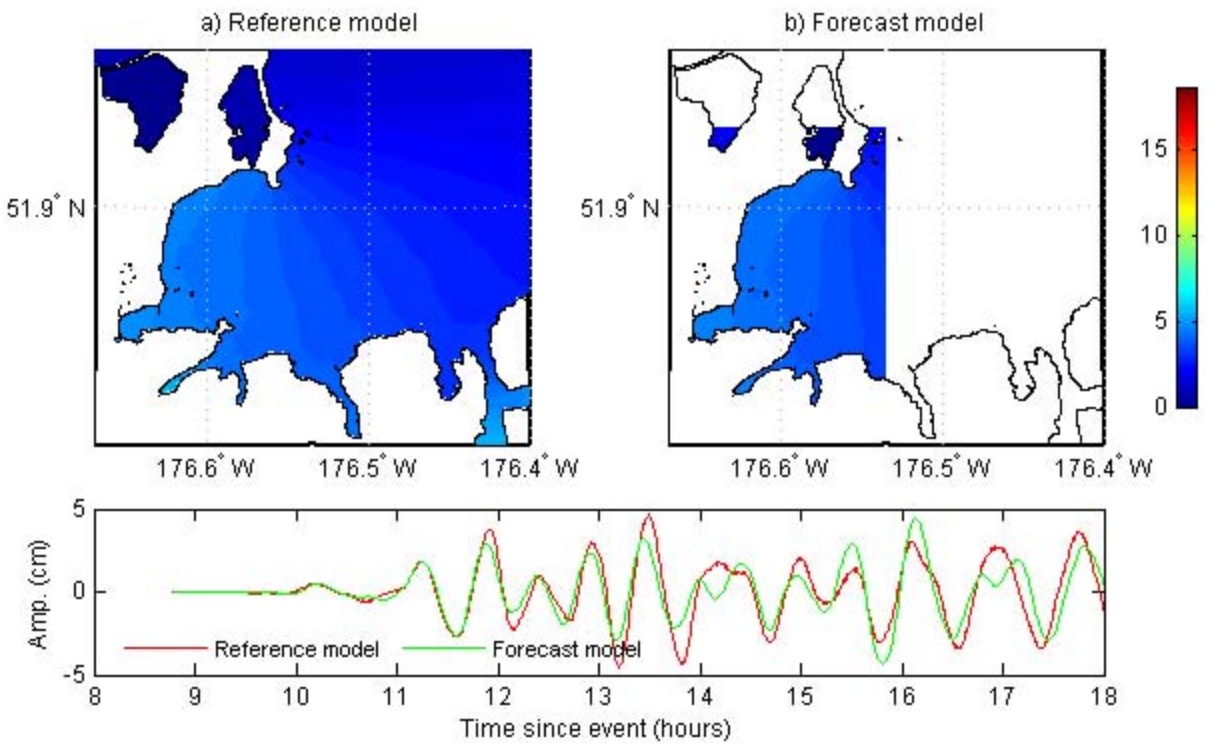
a) Reference model
b) Forecast model
51.9° N
51.9° N
176.6° W
176.5° W
176.4° W
176.6° W
176.5° W
176.4° W
15
10
5
0
Amp. (cm)
5
0
-5
Reference model
Forecast model
8
9
10
11
12
13
14
15
16
17
18
Time since event (hours)

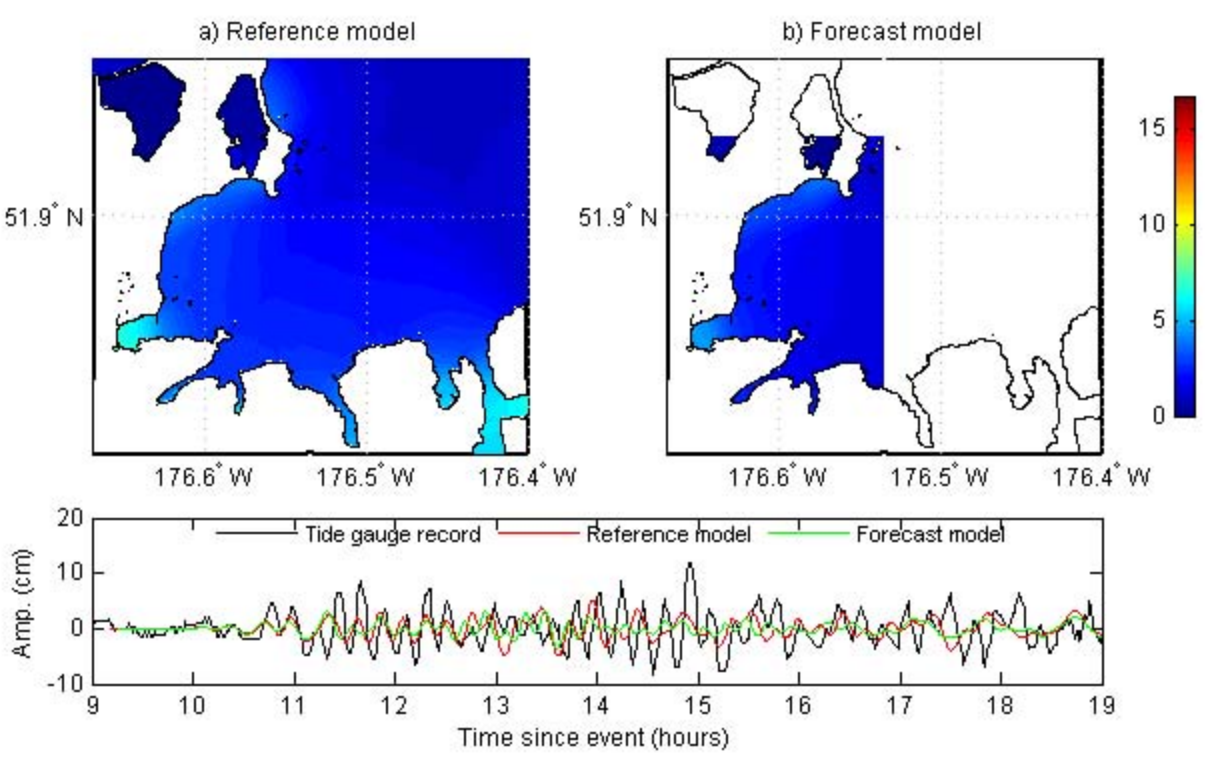
a) Reference model
b) Forecast model
51.9° N
51.9° N
176.6° W
176.5° W
176.4° W
176.6° W
176.5° W
176.4° W
15
10
5
0
Tide gauge record
Reference model
Forecast model
Amp. (cm)
20
10
0
-10
9
10
11
12
13
14
15
16
17
18
19
Time since event (hours)

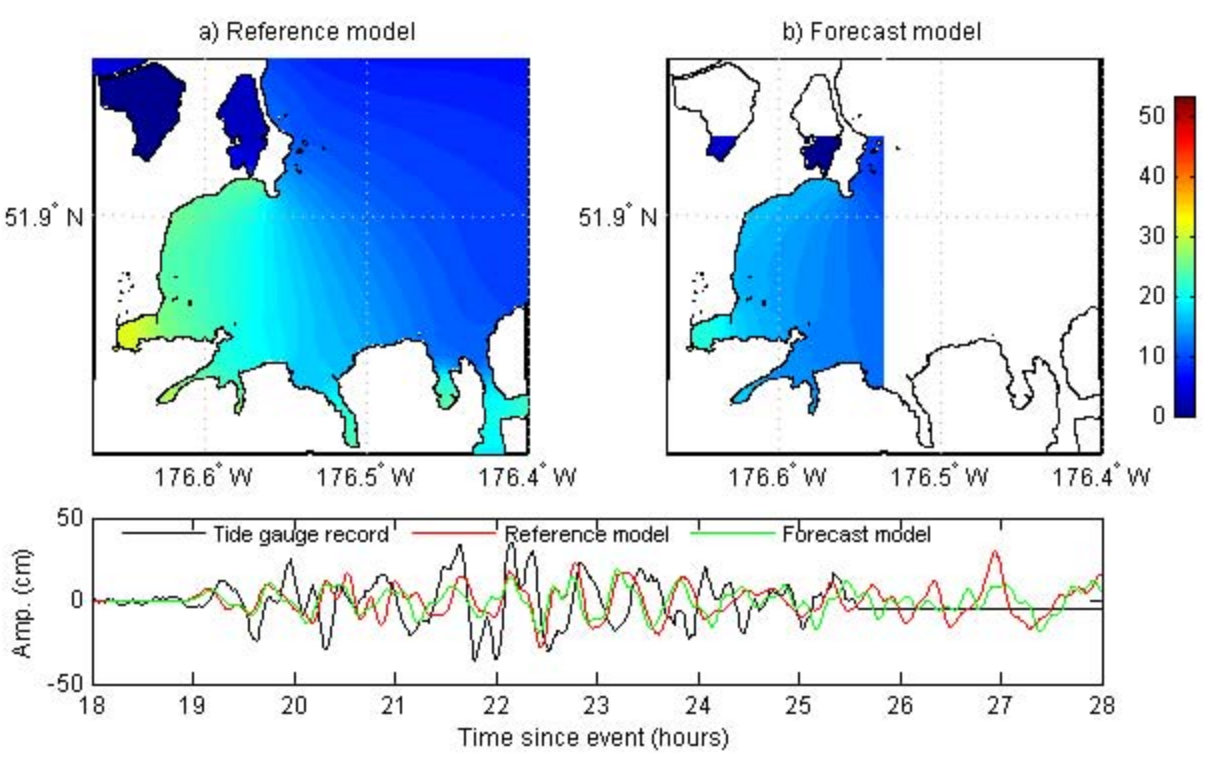
a) Reference model
b) Forecast model
51.9° N
51.9° N
176.6° W
176.5° W
176.4° W
176.6° W
176.5° W
176.4° W
50
40
30
20
10
0
Tide gauge record
Reference model
Forecast model
Amp. (cm)
50
0
-50
18
19
20
21
22
23
24
25
26
27
28
Time since event (hours)

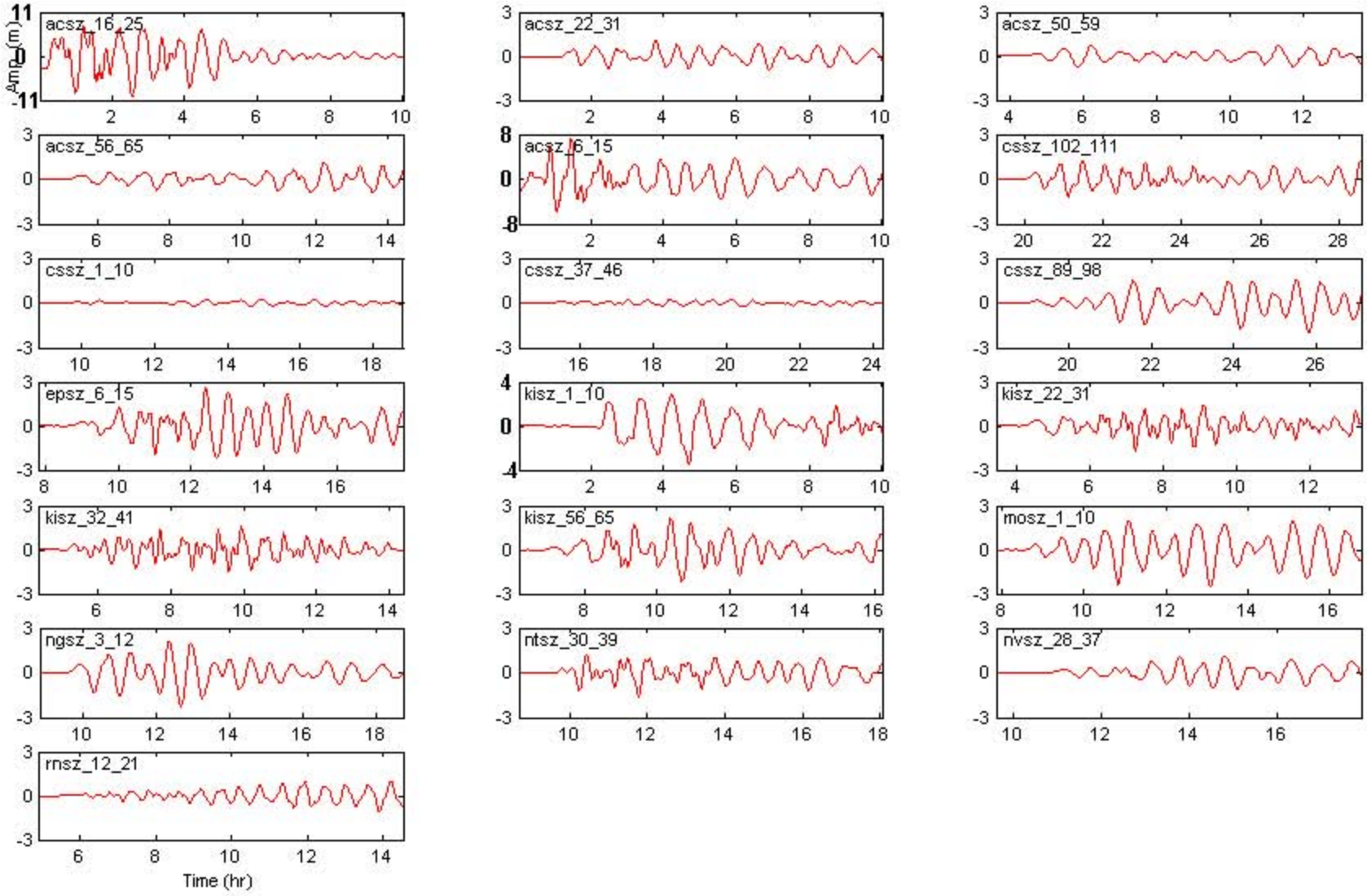
Amp (m)
acsz_16_25
acsz_22_31
acsz_50_59
acsz_56_65
acsz_6_15
cssz_102_111
cssz_1_10
cssz_37_46
cssz_89_98
epsz_6_15
kisz_1_10
kisz_22_31
kisz_32_41
kisz_56_65
mosz_1_10
ngsz_3_12
ntsz_30_39
nvsz_28_37
rnsz_12_21
Time (hr)